JACS
JOURNAL OF THE AMERICAN CHEMICAL SOCIETY

COMMUNICATION

pubs.acs.org/JACS

Membrane-Assisted Online Renaturation for Automated Microfluidic Lectin Blotting

Mei He,[†] Jan Novak,[‡] Bruce A. Julian,[‡] and Amy E. Herr*[,†]

[†]Department of Bioengineering, University of California, Berkeley, California 94720, United States

[‡]Departments of Microbiology and Medicine, University of Alabama, Birmingham, Alabama 35294, United States

Supporting Information

ABSTRACT: Aberrant glycosylation plays a pivotal role in a diverse set of diseases, including cancer. A microfluidic lectin blotting platform is introduced to enable and expedite the identification of protein glycosylation based on protein size and affinity for specific lectins. The integrated multistage assay eliminates manual intervention steps required for slab-gel lectin blotting, increases total assay throughput, limits reagent and sample consumption, and is completed using one instrument. The assay comprises non-reducing sodium dodecyl sulfate polyacrylamide gel electrophoresis (SDS-PAGE) followed by online post-sizing SDS filtration and lectin-based affinity blotting. Important functionality is conferred through both device and assay advances that enable integration of nanoporous membranes flanking a central microchamber to create sub-nanoliter volume compartments that trap SDS−protein complexes and allow electrophoretic SDS removal with buffer exchange. Recapitulation of protein binding for lectin was optimized through quantitative assessment of SDS-treated green fluorescent protein. Immunoglobulin A1 aberrantly glycosylated with galactose-deficient *O*-glycans was probed in ∼6 min using ∼3 μL of sample. This new microfluidic lectin blotting platform provides a rapid and automated assay for the assessment of aberrant glycosylation.

Glycosylation is a post-translational protein modification associated with cell differentiation and normal cellular functions. Abnormal glycosylation of specific glycoproteins has been described in cancer and autoimmune diseases.[1] Aberrant glycosylation has also been associated with disease progression.[2] Despite the potential of glycans as reliable clinical biomarkers, development has been slow. The major delaying factors stem in part from the shortcomings of conventional analytical technology and the natural complexity and heterogeneity of glycosylation.[3] Although lectin-based blots are powerful tools, the labor-intensive, time-intensive, low-throughput nature of the workflow is limiting.[4] While lectin arrays are a promising high-throughput alternative approach for analyzing glycosylation patterns,[5] arrays do not provide information about protein molecular weight (MW). Because of the structural complexity and diversity of glycoproteins, next-generation protein assays would benefit from an automated, high-throughput approach that provides information about glycosylation as well as protein MW.[6]

Recent advances in bioanalytical technology have streamlined and automated blotting techniques. Capillary electrophoresis formats show promise with reduced reagent and time requirements,[7] and fully automated operation (e.g., fluid exchange, sample transfer) and scale-up are underway. Other efforts have focused on scale-up of conventional slab-gel technologies, including polymer gasket technology introduced to create flow channels for application of blocking solutions and multiple antibody probe solutions to poly(vinylidene fluoride) (PVDF) membranes.[8] Although multiplexing is enhanced, the separation and membrane-transfer steps still rely on slow, sample-consuming macroscale slab-gel formats with manual integration of steps. Consequently, unified, automated protein immunoblot techniques would fill a broad and currently unmet analytical need.[9]

Thus, we introduce a unified, fully automated multidimensional assay that integrates sizing (SDS-PAGE) under nonreducing conditions with online full or partial recovery of protein binding capacity and subsequent in-chip lectin blotting (Figure 1). The assay is performed in a glass microfluidic device housing a microchamber and microchannel network (Figure 1A). There are two major considerations in regard to sizing of glycoproteins. First, non-reducing SDS-PAGE retains the global glycoprotein structure and avoids non-specific (false) lectin binding that is sometimes observed under reducing conditions.[10] Second, SDS treatment of proteins in SDS-PAGE has a significant impact on the native protein structure and can reduce binding affinities.[11] Consequently, washing steps to dilute and remove SDS after SDS-PAGE are included as part of slab-gel lectin blot workflows.[12] Microscale handling provides an avenue for efficient protein renaturation in terms of time, materials consumption, and losses (e.g., associated with dilution). Nevertheless, while microchannel networks offer design strategies[13] for reagent metering, mixing, denaturant diffusion, and removal, no effort regarding such on-chip protein manipulation after SDS-PAGE has been reported. In order to address this challenge, we have integrated microscale MW cutoff (MWCO) filters to dilute and remove SDS from resolved protein peaks after non-reducing SDS-PAGE and prior to antibody/lectin blotting (Figure 1B). SDS removal is hypothesized to underpin recapitulation of the binding affinity of previously sized protein species; we call this process "renaturation". Using the integrated workflow, we demonstrate rapid lectin blotting (∼6 min) with limited consumption of sample materials (∼3 μL) and reagents. Introduction of such unified assays advances protein measurement capabilities to meet a broad range of protein analysis challenges spanning from basic sciences to clinical needs.

Received: August 23, 2011
Published: November 09, 2011

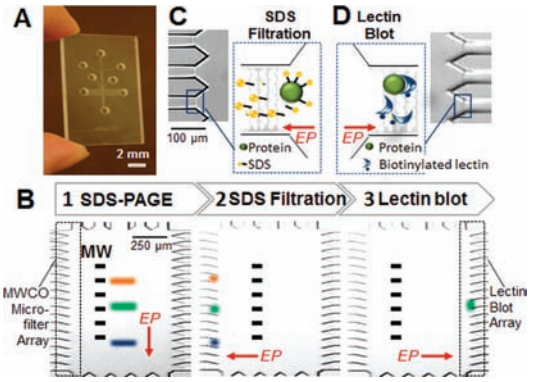

Figure 1. Microfluidic integration of protein separation, intra-assay sample manipulation, and probing with immobilized lectin yields an automated lectin blot. (A) Glass microfluidic device with a microchamber at the center. (B) Schematic illustration of the three assay stages: SDS-PAGE, SDS dilution via microfiltration during protein renaturation, and probing of renatured proteins using biotinylated lectin immobilized to streptavidin acrylamide. "MW" indicates molecular weight. (C) Micrograph of MWCO microfilters used for post-sizing SDS removal. The microfilters exclude transport of species with MW > 20 kDa, thus allowing buffer and SDS to exit the chamber, as indicated in the schematic inset. (D) Biotinylated lectin (or antibody) is housed in streptavidin acrylamide in a microchannel array flanking the right-hand side of the microchamber. Analytes with affinity for immobilized species are retained. All other species electromigrate out of the array. Arrows labeled "*EP*" indicate the direction of electrophoresis.

The MWCO microfilters are polyacrylamide (PA) gel membranes located in a microchannel array flanking the central microchamber. The MWCO microfilters are fabricated using one-step photopatterning of a 45%T PA gel in the channel array (Figure 1C). As a result of their placement in channels, the filters define compartments that allow electrophoresis-assisted lateral buffer exchange and SDS filtration [Figure S1 and Table S1 in the Supporting Information (SI)]. After SDS removal, species are driven to a blotting region flanking the opposite side of the microchamber (Figure 1D). The PA blotting gels incorporate streptavidin acrylamide, which is decorated with biotinylated antibody or lectin. Directed electrophoresis through the 3D reactive "pores" in the blotting region is hypothesized to enhance transport by reducing the diffusion distance and confer improved binding through controlled orientation of the capture reagent[14] (see Figure S2). The use of 2D electric field control in the 0.5 mm × 2 mm gel-patterned microfluidic chamber[9] allows the total blotting workflow to be conducted in one unified microdevice in an automated format (Figure S1 and Table S1).

The MWCO microfilters offer a low-MW cutoff that allows buffer ions and SDS monomers (MW = 288 kDa) to pass out of the microchamber while excluding larger species such as proteins (>20 kDa). The critical micelle concentration (CMC) of SDS is 6−8 mM (~0.23% w/v). Above the CMC, SDS micelles form with a maximum MW of 16 kDa and break up into monomers upon dilution.[15] Both SDS-treated trypsin inhibitor (21 kDa) and green fluorescent protein (GFP, 27 kDa) were empirically determined to be excluded from electromigration through the microfilters (Figure S1). The electrophoretic mobility of SDS micelles is higher than that of the model proteins ($\mu_{SDS} = -6.0 \times 10^{-4}$ cm^2 V^{-1} s^{-1} vs $\mu_{TI} = -2.0 \times 10^{-4}$ cm^2 V^{-1} s^{-1}, both at pH 7.0),[16] so SDS micelles are expected to electromigrate more quickly under the same applied electric field with other conditions held constant. Therefore,

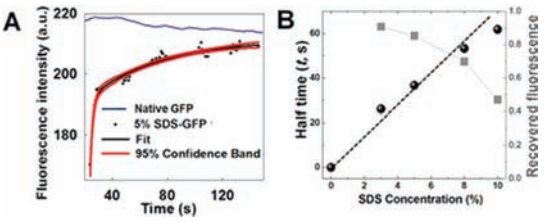

Figure 2. Characterization of the renaturation of 5% SDS-treated GFP during treatment at on-chip MWCO microfilters. (A) Time evolution of the fluorescence signal during treatment and fit to a double-exponential function. The GFP concentration was 200 nM. (B) Renaturation half-time and fluorescence recovery are dependent on the SDS concentration.

the SDS removal process is not expected to be a rate-limiting step for protein renaturation. During the MWCO microfilter sample treatment process, an oscillating voltage is applied to minimize protein entanglement or adsorption to the PA gel constituting the MWCO microfilters (Table S1 and Figure S3).

GFP fluorescence has been correlated with structure, suggesting that monitoring the fluorescence signal of SDS-treated GFP (SDS-GFP) at the microfilters during buffer exchange and SDS removal (recovered fluorescence) should provide one means of evaluating GFP renaturation. To assess the fluorescence recovery of SDS-GFP during manipulation by the MWCO microfilters, a stream (not a zone) of 5% SDS-GFP was electrophoresed into the microchamber and then manipulated at the MWCO microfilters (Figure S1b). Monitoring of the fluorescence recovery for native GFP yielded a gradual decrease in fluorescence signal (Figure 2A). In contrast, the same handling used on 5% SDS-GFP yielded a notable increase in the fluorescence signal, suggesting some degree of GFP renaturation. Double-exponential fits of the recovered fluorescence in handling-time courses for GFP treated with a range of SDS concentrations yielded estimates of both the renaturation rate constant (k) and half-time (t) (see Figure 2B and Table S2).[17] The recovered fluorescence was inversely related to the SDS concentration in the sample, suggesting that less SDS in the initial sample leads to a more effective renaturation process. The GFP renaturation kinetics found here agrees with literature results for conventional dilution-based GFP renaturation.[18] The consistent performance of GFP handling at the MWCO microfilter array is shown in Figure S4. The intra-assay sample handling introduced here allows time-dependent characterization of the renaturation process while incurring minimal sample dilution and material losses. Such characteristics are important for the optimization of assays that combine SDS-PAGE with subsequent probing. Furthermore, to the best of our knowledge, this strategy provides the first demonstration of monitoring of protein refolding kinetics using a microfilter, which is potentially relevant for precious samples.

Information losses inherent in intra-assay sample handling were assessed for the MWCO microfilter approach introduced here, informing both assay and chip design. Here the channel array housing the microfilters was fabricated with pitches of 10 and 50 μm between the channel centerlines. MW protein ladders were transferred from the SDS-PAGE separation axis to the lateral microchannel arrays (Figure S5 and Table S3), with both designs allowing reconstruction of the separation profile from the SDS-PAGE axis. Figure 3 shows that oversampling of the protein zones minimizes deseparation and MW information losses[19] (Figure S6 and Table S3; also see the movie in the SI). In this case, the losses of MW information are ~5 kDa, with separation resolution (SR) losses of <4%.

dx.doi.org/10.1021/ja207963f |*J. Am. Chem. Soc.* 2011, 133, 19610–19613

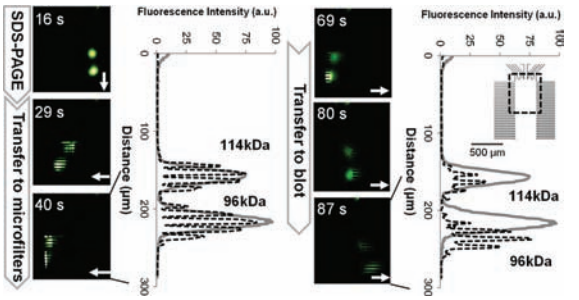

Figure 3. Characterization of transfer losses arising from intra-assay sample handling and treatment. Fluorescence micrographs report the time evolution of the integrated assay for two model proteins [phosphorylase B (96 kDa) and β-galactosidase (114 kDa); 5% SDS treatment]. Plots of the fluorescence intensity distribution on the separation axis (gray lines) are compared with the fluorescence intensity distributions in the MWCO microfilter array (dashed black line at 40 s) and the blotting array (dashed black line at 87 s). Arrows indicate the direction of electrophoresis. The array channel spacing is ~10 um. The chip design and imaging region are shown in the inset.

The unified on-chip lectin blotting assay was used to assess human immunoglobulin A1 (IgA1) aberrantly glycosylated with galactose-deficient *O*-glycans. This IgA1 glycosylation aberrancy is typical for IgA nephropathy (IgAN). IgAN is the most common primary glomerulonephritis, frequently leading to end-stage renal disease.[20] Specifically, *O*-glycans attached to serine and threonine residues in the hinge region of the α1 heavy chain in IgA1 are deficient in galactose and thus have exposed terminal *N*-acetylgalactosamines (GalNAc) (Figure S7). In contrast, normal IgA1 *O*-glycans consist of GalNAc and galactose. On the basis of these observations, aberrantly glycosylated serum IgA1 has been proposed as a glycosylation-associated IgAN biomarker.[20]

Toward this end, we assessed lectin binding to naturally galactose-deficient IgA1 myeloma protein that mimics the aberrancy found in IgA1 from patients with IgAN (see the SI). Lectin from *Helix aspersa* (HAA) is specific for terminal GalNAc on galactose-deficient IgA1[21] and thus was immobilized in the blotting region. Normally glycosylated IgA1 purified from the serum of a healthy individual was used as a negative control (i.e., no interaction with HAA was expected). Conventional HAA lectin slab-gel blotting was performed (Figure S7), and HAA bound to the IgA1 myeloma protein, thus confirming that the *O*-glycans of IgA1 are galactose-deficient. HAA did not bind to IgA1 from normal human serum, supporting the assertion that this IgA1 is normally glycosylated. Notably, a non-specific (false) response under reducing condition was observed.

On-chip non-reducing SDS-PAGE of fluorescently labeled galactose-deficient IgA1 myeloma protein (green) was conducted and yielded an average SR of 1.3 (Figure 4A) for the five species present. The on-chip analysis was consistent with the slab gel (Figure S7) yet required 32 s of separation time. An SDS-PAGE protein ladder (68−200 kDa, labeled with a red fluorophore) was separated simultaneously and observed in a second optical channel (Figure 4A). Two-color monitoring enabled MW calibration for unknown proteins and provided size information via a linear calibration curve (R^2 > 0.96). Size-to-mobility calibration curves were generated for three SDS treatment conditions (3, 5, and 10% SDS; Figure 4A). The 5% SDS treatment was applied for sizing of the galactose-deficient IgA1 myeloma protein. The calibration relation [log(MW) = (−0.13 × mobility) + 2.6] suggested an IgA1 MW of 160 kDa

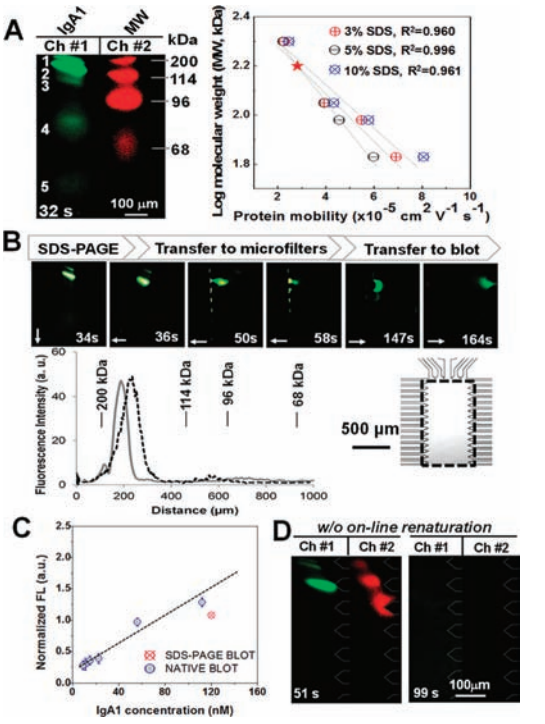

Figure 4. Microfluidic HAA lectin blot of galactose-deficient IgA1 myeloma protein. (A) Fluorescence micrographs show two-color monitoring of MW ladders and myeloma IgA1 sizing. The linear calibration curves (right) were obtained using various concentrations of SDS for calculation of unknown protein MWs [myosin heavy chain (200 kDa), β-galactosidase (114 kDa), phosphorylase B (96 kDa), and human serum albumin (68 kDa)]. The red star indicates the size of monomeric IgA1. (B) Fluorescence micrographs report the time evolution of the HAA lectin blot of galactose-deficient IgA1 myeloma protein. The plot of the fluorescence intensity distribution on the separation axis (gray line) is compared with the intensity distribution in the blotting array (dashed black line at 164 s). Arrows indicate the direction of electrophoresis. The array channel spacing is ~50 μm. The imaging region is shown in the inset. (C) Evaluation of the recovered activity by comparison of the amounts of captured myeloma IgA1 in the blotting region under native and SDS conditions. (D) HAA blot of 5% SDS-treated myeloma IgA1 (green) and MW ladders (68−200 kDa, red) without online renaturation, as a negative control.

(Figure 4A), consistent with the expected MW of monomeric IgA1. The sizes of species 3 and 4 were assigned as 141 and 85 kDa, respectively, and these species were hypothesized to be fragments of IgA. Species 3 is consistent with the 141 kDa monomer lacking one light chain (L), whereas the 85 kDa species 4 is consistent with H (heavy chain)1+L1. Species 3 and 4 were observed with slab-gel sizing (Figure S7). Species 5 was assigned as free dye (<1 kDa).

After non-reducing SDS-PAGE, species were laterally transferred into the flanking MWCO microfilters for SDS removal and buffer exchange by applying a transfer potential for 100 s, as described previously. Treated protein species were then electrophoresed across the chamber and into the blotting region (Figure 4B). The losses of MW information from the SDS-PAGE axis to the final blot axis were ~7 kDa, with SR losses of <5%.

The role of on-chip renaturation and SDS removal in recapitulating lectin recognition of sized proteins was estimated by comparing on-chip lectin blotting of native IgA1 (no SDS present) to blotting of SDS-treated and subsequently renatured IgA1(Figure 4C). The fluorescence signal of protein retained in

the HAA blotting region suggests ~75% recovery of the lectin-binding capacity for SDS-treated proteins using the MWCO microfilter approach (Figure 4C). This binding capacity performance is sufficient for assays of serum IgA1, which is the dominant subclass of total serum IgA (>2 mg/mL).[22]

To assess the role of SDS dilution in recapitulating the lectin binding affinity, we performed lectin blotting of SDS-treated IgA1 without on-chip renaturation and SDS dilution (Figure 4D). Here 5% SDS-myeloma IgA1 was directly transferred to the blotting region after on-chip SDS-PAGE, with no treatment at the MWCO microfilters. As expected, no detectable binding was observed. Likewise, transfer of a MW ladder (68−200 kDa) to the HAA blotting region showed no appreciable binding, suggesting negligible non-specific adsorption and size-exclusion effects (Figure 4D). The microfluidic HAA lectin blot allowed a rapid (~6 min) assessment of IgA1 *O*-linked galactose deficiency that mimics serum IgA1 from patients with IgAN.

We have demonstrated a rapid and automated assay comprising SDS-PAGE, in situ renaturation and SDS-dilution, electrophoretic transfer between stages, and subsequent affinity blotting in a single microfluidic device. An array of MWCO microfilters enables SDS removal between the sizing and blotting stages and allows recapitulation of the binding affinity for proteins after SDS sizing. Subsequent antibody probing of lectin-captured glycosylated proteins (labeled or unlabeled) is feasible and would yield a lectin−glycoprotein−antibody sandwich reporting the protein size, glycosylation status, and immunoreactivity.[23] While the targeted proteomic assay detailed here has been developed for analysis of IgA1, the assay format makes both the operational parameters (separation field strength, buffer constituents) and the device parameters (separation length, separation-gel pore size distribution, geometry and length scales of flanking arrays)[24] readily adjustable to other assays of interest. Analysis of purified and fluorescently labeled targets enabled performance characterization during development (i.e., total assay losses and the on-chip renaturation process), and application to unlabeled and crude samples is promising and currently underway. Previous studies have demonstrated compatible formats for on-chip sandwich probing with free labeling of antigen targets and robust analysis of minimally processed complex biological fluids (i.e., serum, tear fluid, and saliva), thus pointing to maturation paths for the total integration of sample preparation.[25] Multiplexing and throughput scale up in both parallel and serial workflows is also under development.[23] The assay and device advances detailed in the present study form a foundation for maturation of the approach to aid in the investigation of a diverse set of diseases where glycosylation is suspected to play an important role.

■ ASSOCIATED CONTENT

Supporting Information. Procedures, additional results, complete ref 7b, and a movie showing the total assay. This material is available free of charge via the Internet at http://pubs.acs.org.

■ AUTHOR INFORMATION

Corresponding Author
aeh@berkeley.edu

■ ACKNOWLEDGMENT

The authors acknowledge financial support from the UC Discovery Program and the Industry−University Cooperative Research Program (IUCRP). Partial infrastructure support was provided by the QB3 Biomolecular Nanofabrication Center (BNC). J.N. and B.A.J. were supported in part by NIH Grants DK078244, DK082753, DK083663, DK075868, GM098539, and DK071802. A.E.H. is an Alfred P. Sloan Research Fellow.

■ REFERENCES

(1) Fuster, M. M.; Esko, J. D. *Nat. Rev. Cancer* **2005**, *5*, 526.
(2) Reis, C. A.; Osorio, H.; Silva, L.; Gomes, C.; David, L. *J. Clin. Pathol.* **2010**, *63*, 322.
(3) Lebrilla, C. B.; An, H. J. *Mol. BioSyst.* **2009**, *5*, 17.
(4) Hirabayashi, J. *J. Biochem.* **2008**, *144*, 139.
(5) (a) Pilobello, K. T.; Slawek, D.; Mahal, L. K. *Proc. Natl. Acad. Sci. U.S.A.* **2007**, *104*, 10534. (b) Kuno, A.; Uchiyama, N.; Koseki-Kuno, S.; Ebe, Y.; Takashima, S.; Yamada, M.; Hirabayashi, J. *Nat. Methods* **2005**, *2*, 851.
(6) Bosques, C. J.; Raguram, S.; Sasisekharan, R. *Nat. Biotechnol.* **2006**, *24*, 1100.
(7) (a) Anderson, G. J.; Cipolla, C. M.; Kennedy, R. T. *Anal. Chem.* **2011**, *83*, 1350. (b) O'Neill, R. A.; et al. *Proc. Natl. Acad. Sci. U.S.A.* **2006**, *103*, 16153. (c) Lu, J. J.; Zhu, Z.; Wang, W.; Liu, S. *Anal. Chem.* **2011**, *83*, 1784.
(8) Pan, W.; Chen, W.; Jiang, X. *Anal. Chem.* **2010**, *82*, 3974.
(9) (a) He, M.; Herr, A. E. *J. Am. Chem. Soc.* **2010**, *132*, 2512. (b) He, M.; Herr, A. E. *Nat. Protoc.* **2010**, *5*, 1844.
(10) Kuizenga, A.; Haeringen, A. J. V.; Kijlstra, A. *Invest. Ophthalmol. Vis. Sci.* **1991**, *32*, 3277.
(11) Jaenicke, R. *Angew. Chem., Int. Ed. Engl.* **1984**, *23*, 395.
(12) Walker, J. M. *The Protein Protocols Handbook*; Humana Press: New York, 2002; Part VI, pp 779−793.
(13) (a) Kondapalli, S.; Kirby, B. J. *Microfluid. Nanofluid.* **2009**, *7*, 275. (b) Zaccai, N. R.; Yunus, K.; Matthews, S. M.; Fisher, A. C.; Falconer, R. J. *Eur. Biophys. J.* **2007**, *36*, 581. (c) Yamaguchi, H.; Miyazaki, M.; Briones-Nagata, M. P.; Maeda, H. *J. Biochem.* **2010**, *147*, 895.
(14) Propheter, D. C.; Hsu, K.; Mahal, L. K. *ChemBioChem* **2010**, *11*, 1203.
(15) Bales, B. L.; Messina, L.; Vidal, A.; Peric, M. *J. Phys. Chem. B* **1998**, *102*, 10347.
(16) Takeda, K.; Sasaoka, H.; Sasa, K.; Hirai, H.; Hachiya, K.; Moriyama, Y. *J. Colloid Interface Sci.* **1992**, *154*, 385.
(17) Enoki, S.; Saeki, K.; Maki, K.; Kuwajima, K. *Biochemistry* **2004**, *43*, 14238.
(18) Pédelacq, J.; Cabantous, S.; Tran, T.; Terwilliger, T. C.; Waldo, G. S. *Nat. Biotechnol.* **2006**, *24*, 79.
(19) Murphy, R. E.; Schure, M. R.; Foley, J. P. *Anal. Chem.* **1998**, *70*, 1585.
(20) Suzuki, H.; Moldoveanu, Z.; Hall, S.; Brown, R.; Vu, H. L.; Novak, L.; Julian, B. A.; Tomana, M.; Wyatt, R. J.; Edberg, J. E.; Alarcón, G. S.; Kimberly, R. P.; Tomino, Y.; Mestecky, J.; Novak, J. *J. Clin. Invest.* **2008**, *118*, 629.
(21) Moore, J. S.; Kulhavy, R.; Tomana, M.; Moldoveanu, Z.; Suzuki, H.; Brown, R.; Hall, S.; Kilian, M.; Poulsen, K.; Mestecky, J.; Julian, B. A.; Novak, J. *Mol. Immunol.* **2007**, *44*, 2598.
(22) Jones, C.; Mrmelstein, N.; Smith, P. K.; Powell, H.; Roberton, D. *Clin. Exp. Immunol.* **1988**, *72*, 344.
(23) Tia, S. M.; He, M.; Kim, D.; Herr, A. E. *Anal. Chem.* **2011**, *83*, 3581.
(24) Lerch, M. A.; Hoffman, M. D.; Jacobson, S. C. *Lab Chip* **2008**, *8*, 316.
(25) (a) Yamada, M.; Mao, P.; Fu, J.; Han, J. *Anal. Chem.* **2009**, *81*, 7067. (b) Karns, K.; Herr, A. E. *Anal. Chem.* **2011**, *83*, 8115. (c) Herr, A. E.; Hatch, A. V.; Throckmorton, D. J.; Tran, H. M.; Brennan, J. S.; Giannobile, W. V.; Singh, A. K. *Proc. Natl. Acad. Sci. U.S.A.* **2007**, *104*, 5268.